Muscle metabolic and neuromuscular determinants of fatigue during cycling in different exercise intensity domains

Original Investigation

Matthew I. Black[1 2], Andrew M. Jones[1], Jamie R. Blackwell[1], Stephen J. Bailey[1 2], Lee J. Wylie[1], Sinead T.J. McDonagh[1], Christopher Thompson[1], James Kelly[1], Paul Sumners[3], Katya J. Mileva[3], Joanna L. Bowtell[1], Anni Vanhatalo[1]

[1]College of Life and Environmental Sciences, St. Luke's Campus, University of Exeter, Heavitree Road, Exeter, EX1 2LU, United Kingdom. [2]School of Sport, Exercise and Health Sciences, Loughborough University, Epinal Way, LE11 3TU, United Kingdom. [3]Sport and Exercise Science Research Centre, School of Applied Sciences, London South Bank University, 103 Borough Road, London, SE1 0AA, United Kingdom.

Running head: Metabolic and neuromuscular correlates of fatigue

Correspondence:

Anni Vanhatalo, Ph.D.

E-mail: a.vanhatalo@exeter.ac.uk

Tel: 01392 722815

Fax: 01392 264726

ABSTRACT

The lactate or gas exchange threshold (GET) and the critical power (CP) are closely associated with human exercise performance. We tested the hypothesis that the limit of tolerance (T_{lim}) during cycle exercise performed within the exercise intensity domains demarcated by GET and CP is linked to discrete muscle metabolic and neuromuscular responses. Eleven males performed a ramp incremental exercise test, 4-5 severe-intensity (SEV; >CP) constant-work-rate (CWR) tests until T_{lim}, a heavy-intensity (HVY; <CP but >GET) CWR test until $T_{lim,}$ and a moderate-intensity (MOD; <GET) CWR test until T_{lim}. Muscle biopsies revealed that a similar (P>0.05) muscle metabolic milieu (i.e., low pH and [PCr] and high [lactate]) was attained at T_{lim} (~2-14 min) for all SEV exercise bouts. The muscle metabolic perturbation was greater at T_{lim} following SEV compared to HVY, and also following SEV and HVY compared to MOD (all P<0.05). The normalised M-wave amplitude for the m. vastus lateralis (VL) decreased to a similar extent following SEV (-38±15%), HVY (-68 ± 24%), and MOD (-53±29%), (P>0.05). Neural drive to the VL increased during SEV (4±4%; P<0.05) but did not change during HVY or MOD (P>0.05). During SEV and HVY, but not MOD, the rates of change in M-wave amplitude and neural drive were correlated with changes in muscle metabolic ([PCr], [lactate]) and blood ionic/acid-base status ([lactate], [K^+]) (P<0.05). The results of this study indicate that the metabolic and neuromuscular determinants of fatigue development differ according to the intensity domain in which the exercise is performed.

NEW AND NOTEWORTHY

The gas exchange threshold and the critical power demarcate discrete exercise intensity domains. For the first time, we show that the limit of tolerance during whole-body exercise within these domains is characterized by distinct metabolic and neuromuscular responses. Fatigue development during exercise >CP is associated with the attainment of consistent 'limiting' values of muscle metabolites whereas substrate availability and limitations to muscle activation may constrain performance at lower intensities.

KEYWORDS

Critical power; gas exchange threshold; neuromuscular fatigue; muscle metabolism; cycling exercise

INTRODUCTION

Intense and/or prolonged excitation of muscle leads to a reversible decline in its force generating capacity and rate of contraction, commonly known as fatigue (21, 22, 23, 55, 27). This temporary reduction in muscle performance may be attributed to central factors that limit the neural drive for muscle contraction, and to peripheral factors, which occur at, or distal to, the neuromuscular junction and that often involve metabolic and ionic perturbations that reduce the muscle's ability to respond to neural stimulation (2, 3, 25, 30, 41).

The extent of the muscle metabolic and ionic, and blood acid-base and respiratory perturbations experienced during exercise is dependent on the exercise intensity, which can be categorised into three distinct domains demarcated by physiological thresholds (32, 72). The upper limit of the 'moderate' exercise intensity domain is indicated by the lactate threshold (LT; which is often estimated using the gas exchange threshold (GET)), and the boundary between the 'heavy' and 'severe' exercise intensity domains is given by the critical power (CP). Using ^{31}P-magnetic resonance spectroscopy (^{31}P-MRS), it has been demonstrated that severe-intensity, single-leg knee-extension exercise is associated with a progressive loss of muscle homeostasis with time (i.e. progressive reductions in muscle phosphocreatine concentration ([PCr]) and pH and an increase in inorganic phosphate concentration ($[P_i]$)) (9, 31, 33, 69). In contrast, heavy- and moderate-intensity, small muscle mass exercise is associated with much more limited muscle metabolic perturbation with new 'steady-state' values of [PCr], pH and $[P_i]$ being achieved within a few minutes of the initiation of exercise (33, 48, 67). These intensity-related differences in muscle metabolic, as well as related blood acid-base and respiratory gas exchange, responses to exercise (33, 51,

68, 73) likely underpin the close relationships reported between these threshold phenomena (LT/GET and CP) and human exercise performance (8).

The role of exercise intensity in defining the extent and dynamics of muscle metabolic perturbation implies that exercise intensity may also influence the nature of neuromuscular fatigue development (3, 22, 24, 39, 41, 52, 53). The peripheral component to fatigue, as estimated non-invasively using surface electromyography (EMG), electrical muscle stimulation and/or transcranial magnetic stimulation, appears to be especially important during high-intensity exercise (45, 64, 66), whereas central fatigue may be more prominent during prolonged, low-intensity exercise (38, 45, 57, 61, 66). The intensity-dependent interaction between peripheral and central components of fatigue is thought to be modulated by changes in afferent feedback arising from the muscle metabolic milieu. Consistent with this, the critical torque (CT; analogous with the CP) for small muscle mass exercise has been shown to represent a threshold in the development of neuromuscular fatigue (10), such that severe-intensity knee-extensor contractions (>CT) were associated with elevated motor unit recruitment and a disproportionate increase in the rate of neuromuscular fatigue development relative to heavy-intensity contractions (<CT).

It is presently unclear whether the determinants of neuromuscular fatigue development during whole-body exercise, such as cycling, differ according to the intensity domain in which exercise is performed. Previous studies have assessed neuromuscular fatigue before and after self-paced maximal time trial cycle exercise (66) and during constant-work-rate (CWR) cycling performed ostensibly within the severe-intensity domain (65). These studies suggested that, in contrast to knee extension exercise (10), the level of peripheral fatigue at exhaustion for cycling may also be intensity-dependent above CP (65). Compared to small

muscle mass exercise, whole-body exercise is associated with greater rates of pulmonary ventilation and gas exchange (58, 74), differences in cardiac output and muscle perfusion (12, 46, 58), and greater activity of type III/IV muscle afferents that may modulate central drive (52, 53). It is possible that these factors impact the relationship between muscle metabolic changes and neuromuscular fatigue development during exercise.

To date, the physiological and neuromuscular responses to whole-body exercise, and their possible inter-relationship, has not been assessed within distinct exercise intensity domains. The purpose of this study was therefore to evaluate possible differences in the muscle metabolic and systemic responses to different, well-defined, intensities of exercise, with the aim of elucidating whether the exercise intensity domain influences the determinants of neuromuscular fatigue. Based on earlier studies investigating small muscle mass exercise (33, 69), we tested the hypotheses that: 1) a consistent muscle metabolic milieu ([ATP], [PCr], [lactate], pH) and neuromuscular responses (muscle excitability and neural drive) will be attained at the limit of tolerance (T_{lim}) during severe-intensity exercise (>CP); 2) severe-intensity exercise will be associated with greater muscle metabolic perturbation compared to heavy- and moderate-intensity exercise; and 3) the rate of neuromuscular fatigue development will be greater during severe- compared to heavy- and moderate-intensity exercise due to greater muscle metabolic and ionic perturbations.

METHODS

Ethical approval

The protocols were approved by the host institution's Research Ethics Committee and conducted in accordance with the code of the ethical principles of the World Medical

Association (Declaration of Helsinki). Subjects gave written informed consent to participate after the experimental procedures, associated risks, and potential benefits of participation had been explained.

Subjects

Eleven healthy recreationally active males (mean ± SD: age 21.8 ± 1.9 years, height 1.79 ± 0.05 m, body mass 78.2 ± 8.1 kg) volunteered to participate in this study, 8 of whom volunteered to provide muscle tissue samples. One of the subjects who volunteered for the biopsy procedure withdrew from the study having completed only the severe-intensity exercise trials. This subject's data were excluded from statistical difference tests, but included in the correlational analysis. All subjects were in good health and had no known history of neurological or motor disorder. Subjects were instructed to report to all testing sessions in a rested and fully hydrated state, ≥3 h post-prandial, and to avoid strenuous exercise and refrain from caffeine and alcohol in the 24 h prior to testing. Each subject started each experimental trial at the same time of day (±2 h). All trials were performed on the same electronically-braked cycle ergometer (Lode, Excalibur, Groningen, The Netherlands).

Experimental design

Each subject visited the laboratory on ~7 occasions over a 6-wk period with each visit separated by a minimum of 24 h. A minimum of 7 days recovery was provided following the heavy- and moderate-intensity exercise tests. After the completion of a ramp incremental test (visit 1), subjects performed 4-5 CWR severe-intensity exercise tests to define the power-duration relationship, a heavy-intensity CWR test and a moderate-intensity CWR test, completed in a randomised order (Figure 1) except that the severe-intensity tests always preceded the heavy-intensity test. Pulmonary gas exchange was measured continuously

during all tests, with the exception of the moderate-intensity test in which it was measured periodically for 10 min intervals, with the mid-point of collection coinciding with blood sample collection and femoral nerve stimulation (see below). We encouraged the subjects to continue exercising during the moderate-intensity test to enable 10 min of gas exchange data to be collected immediately prior to exercise cessation. EMG data were obtained continuously from m. vastus lateralis (VL) and m. vastus medialis (VM) throughout the exercise period with stimulation of the femoral nerve delivered at regular intervals (Figure 1) to quantify the neuromuscular changes occurring during the exercise protocols. Venous blood samples were obtained before and during exercise for the moderate-, heavy-, and for three of the severe-intensity exercise tests. In addition, muscle tissue was obtained at rest, and immediately following the moderate-, heavy-, and three of the severe-intensity exercise tests (Figure 1). The severe-intensity tests were performed at 3-5 different work-rates (spanning 60%Δ to $\dot{V}_{O_2}$peak; (where Δ refers to the work-rate difference between the GET and the $\dot{V}_{O_2}$peak). Three of these severe-intensity tests (including short 85 ± 5%Δ, intermediate 75 ± 5%Δ, and long 65 ± 5%Δ) were grouped and compared to test for differences in muscle, neuromuscular, and blood responses within the severe-intensity domain.

Incremental test

On the first laboratory visit, subjects completed a ramp incremental test for the determination of the $\dot{V}_{O_2}$peak and gas exchange threshold (GET). The ergometer seat height and handlebars were adjusted for comfort and the same settings were replicated for each subsequent test. Initially, subjects completed 3 min of baseline cycling at 20 W, after which the work-rate was increased by 30 W·min^{-1} until volitional exhaustion. The subjects cycled at a constant self-selected pedal rate (80 rpm, n = 9, 90 rpm, n = 2), which was recorded and reproduced in subsequent tests. The test was terminated when the pedal rate fell more than 10 rpm below

184 the preferred value for more than 5 s despite strong verbal encouragement. Breath-by-breath
185 pulmonary gas exchange data were collected continuously throughout the test and recorded as
186 10-s moving average for data analysis. $\dot{V}O_2$peak was determined as the highest mean $\dot{V}O_2$
187 during any 30-s period and the GET was determined as previously described (5, 68).
188
189 *CWR tests*
190 All CWR tests started with 3 min of cycling at 20 W, followed by a step increase to the
191 required work-rate. Subjects were instructed to remain seated and to maintain their preferred
192 pedal rate for as long as possible. Strong verbal encouragement was provided, but subjects
193 were not informed of either the work-rate or the elapsed time. The tests were terminated
194 when pedal rate fell more than 10 rpm below the preferred value for more than 5 s. The T_{lim}
195 was recorded to the nearest second.
196
197 The parameters of the power-duration relationship (CP and W′) were estimated by
198 completion of 4-5 severe-intensity exercise tests (4 trials, n = 9; 5 trials n = 2) at different
199 work-rates (approximately 60%Δ, 70%Δ, 80%Δ and 100% $\dot{V}_{O_2}$peak) resulting in T_{lim} ranging
200 between approximately 2 and 14 min. If the standard errors associated with the CP and W′
201 exceeded 5 and 10 %, respectively, after four exercise tests had been completed, a fifth test
202 was performed. Any tests in which the end-exercise $\dot{V}_{O_2}$ was <95% of the individual's ramp
203 test determined $\dot{V}_{O_2}$peak were excluded from the modelling of the power-duration
204 relationship.
205
206 The CP and W′ (the amount of work done above the CP) parameters were estimated using
207 three models: the hyperbolic P-T_{lim} model (Equation 1); the linear work-time (W-T_{lim}) model,

where the total work done (W) is plotted against time (Equation 2); and the linear inverse-of-time ($1/T_{lim}$) model, where power output is plotted against the inverse of time (Equation 3):

$$T_{lim} = W' / (P - CP) \quad [1]$$

$$W = CP \cdot T_{lim} + W' \quad [2]$$

$$P = W' (1/ T_{lim}) + CP \quad [3]$$

The standard errors of the estimate associated with the CP and W′ were expressed as coefficients of variation (CV%, i.e. relative to the parameter estimate). For each individual, the 'best fit' model associated with the lowest CV% for CP and W′ was used for further analyses (7).

The work-rate for the heavy-intensity CWR trial was equal to the lower bound of the 95% confidence limit in the CP parameter (33). The moderate-intensity CWR trial was performed at a work-rate corresponding to 90% of the GET. Subjects were permitted to ingest water *ad libitum* during the heavy- and moderate-intensity tests.

Pulmonary gas exchange

Breath-by-breath pulmonary gas exchange and ventilation were measured continuously during all exercise tests, with the exception of the moderate-intensity test, where it was measured at discrete time points (Figure 1). Subjects wore a nose clip and breathed through a mouthpiece and impeller turbine assembly (Jaeger Triple V, Jaeger, Hoechberg, Germany). The inspired and expired gas volume and concentration signals were continuously sampled at 100 Hz (Oxycon Pro, Jaeger, Hoechberg, Germany) via a capillary line connected to the mouthpiece. The gas analysers were calibrated before each trial with gases of known

concentration and the turbine volume transducer was calibrated using a 3-L syringe (Hans Rudolph, Kansas City, MO). The volume and concentration signals were time aligned by accounting for the delay in capillary gas transit and the analyser rise time relative to the volume signal.

Blood analyses

Venous blood samples were drawn into 5-mL heparinised syringes (Terumo Corporation, Leuven, Belgium) from a cannula (Insyte-W™, Becton-Dickinson, Madrid, Spain) inserted into the subject's antecubital vein. The blood was analysed for [lactate] and [glucose] within ~5 min of collection (YSI 2300, Yellow Springs Instruments, Yellow Springs, OH). The remaining whole blood was then centrifuged at 4,000 rpm for 7 min (Hettich EBA 20, Germany) before plasma was extracted and analysed for [K^+] (9180 Electrolyte Analyser, F. Hoffman-La Roche, Basel, Switzerland).

Neuromuscular Function

EMG was used to continuously record the VL and VM activity during exercise, using active bipolar bar electrodes with single differential configuration (DE2.1, DelSys Inc, Boston, MA, USA), positioned over the muscle belly (SENIAM guidelines). The ground electrode was positioned on the patella. Double-sided adhesive interfaces and hypoallergenic medical tape were used to keep the EMG sensors in place and to reduce skin impedance. The leads connected to the electrodes were secured using hypoallergenic medical tape to minimise artefacts due to movement of the leads. The skin area underneath each electrode was shaved, abraded, and cleaned with alcohol swabs prior to electrode placement to minimise skin impedance. The EMG signal was considered of good quality when the average rectified EMG baseline level for each muscle was below 2 μV (18). The EMG signals were pre-amplified

(1,000x), band-pass filtered (20-450 Hz, Bagnioli-8, DelSys Inc, Boston, MA), and digitised at a sampling rate of 2,000 Hz and resolution of 16 bits using a Power 1401 mk-II analog-to-digital converter and Spike 2 data collection software run by custom written sampling configuration (CED, Cambridge Electronic Design, UK).

The location of the optimal site for transcutaneous femoral nerve stimulation was determined whilst the subject was positioned on the cycle ergometer. Using an adhesive cathode (Boots UK Ltd, Nottingham, England) placed approximately 2 cm medial of the femoral pulse, and an adhesive anode (Boots UK Ltd, Nottingham, England) placed at the anterior aspect of the iliac crest, single electrical pulses generated by a constant current stimulator (DS7 A, Digitimer Ltd, UK) were delivered. The cathode was systematically moved vertically and horizontally and the amplitude of the compound muscle action potential (CMAP, M-wave) was monitored to identify the optimal position of the cathode for attaining maximal peak-to-peak M-wave amplitude during the cycling trials.

Following the attachment of the EMG and the stimulation electrodes, the crank angle at which stimulation was to be delivered during the trials was determined for each subject. The subject was positioned on the cycle ergometer and cycled at a moderate work-rate (20 W below GET) for 1 min. The EMG activity obtained during this period was rectified and averaged for 20 complete crank revolutions. The duration of each revolution was determined by a custom-made magnetic switch that generated an event marker signal on each occasion that the crank passed top dead centre (i.e. 0º). For each subject, the crank angle at which the rectified VL EMG activity was maximal was determined, and as performed by Sidhu et al (56) stimulations were delivered at the identified crank angle for all subsequent trials for that participant (65 ± 5° relative to the top dead centre). A custom written sequencer script

triggered 3 stimulations, with at least 1 and up to 10 pedal revolutions between stimuli. The intervals were randomly determined using a random number generator incorporated within the sequencer script. This was designed to prevent participants from anticipating the stimulus delivery, which may affect the evoked response.

A standard M-wave recruitment curve protocol was completed during each laboratory visit. The subject cycled at 20 W below GET throughout the recruitment curve protocol. A single-pulse electrical stimulation (200 μs) was delivered at the individually identified crank angle as described above. The current was increased in 20 mA increments until the M-wave amplitude plateaued at the maximal M-wave amplitude (M_{max}). A pulse of 130% M_{max} current was applied during the exercise tests (mean stimulation intensity: 350 ± 50 mA).

The EMG signals from the VL and VM were processed using a custom written script to measure peak-to-peak M-wave amplitude and M-wave area. The root-mean-square (RMS) of the EMG signal (an index of the power of the signal) was calculated as the mean over a 25 ms pre-stimulation period at each stimulation time point. The EMG RMS amplitudes and the M-wave parameters were normalised to the corresponding values attained after 1 min of exercise during each trial to evaluate temporal changes in the voluntary muscle activation level (i.e. the EMG RMS amplitude) and the peripheral neuromuscular excitability (i.e. the M-wave amplitude and area). In addition, the voluntary EMG RMS amplitude was normalised to the M-wave amplitude recorded at that time point to assess changes in neural drive (RMS/M; 42). The rates of change in M-wave and EMG parameters from baseline cycling to T_{lim} were calculated for each exercise to quantify the rate of neuromuscular fatigue development in each intensity domain.

Muscle biopsy

The biopsy site was prepared on the alternate thigh to the EMG and peripheral nerve stimulation setup. Local anaesthesia was applied (2-3 ml of 20 $mg.ml^{-1}$ lidocaine) and an incision was made in the medial region of the VL. Muscle samples were obtained using needle biopsy with suction (6). Resting muscle samples were obtained prior to any exercise on the first laboratory visit and post-exercise biopsies were taken within ~10 s of the cessation of each exercise test with the subject supported on the ergometer. The muscle tissue was rapidly frozen in liquid nitrogen.

Muscle tissue analysis

The frozen muscle samples from each biopsy were weighed before and after freeze-drying to determine water content. After freeze-drying, the muscle samples were dissected free from blood, fat and connective tissue. Prior to muscle metabolite analysis, 200 µl of 3 M perchloric acid was added to approximately 2.5 mg d.w. muscle. The solution was then centrifuged and placed on ice for 30 min. It was subsequently neutralised to pH 7.0 with 255 µl of cooled potassium bicarbonate ($KHCO_3$) and centrifuged (10,000 *g*). The supernatant was analysed for PCr, ATP and lactate by fluorometric assays (35). An aliquot containing 1-2 mg d.w. muscle was extracted in 1 M hydrochloric acid (HCl) and hydrolysed at 100ºC for 3 h before glycogen content was determined using the hexokinase method (35). Muscle pH was measured using a glass electrode following the homogenisation of 1-2 mg d.w. of muscle in a non-buffering solution containing 145 mM KCl, 10 mM NaCl and 5 mM iodoacetic acid.

Statistical analyses

One-way ANOVAs with repeated measures were used to assess differences between severe-intensity exercise tests in $\dot{V}O_2$peak, muscle [ATP], [PCr], [pH], [lactate], and [glycogen], M-

wave amplitude, M-wave area, voluntary EMG amplitude and RMS/M, and blood and plasma variables at T_{lim}. The data from the severe-intensity tests were subsequently averaged for each individual for comparison with the heavy- and moderate-intensity tests. Differences in $\dot{V}O_2$peak, muscle [ATP], [PCr], [pH], [lactate], and [glycogen] between the severe-, heavy- and moderate-intensity tests were assessed using one-way ANOVAs. Two-way repeated measures ANOVAs (condition x time) were used to analyse differences in M-wave amplitude and area, and voluntary EMG amplitude for the VL and VM, and blood and plasma variables at common time-points (baseline, 1 min, 3 min and T_{lim}) among the severe-, heavy-, and moderate-intensity tests. Significant interaction and main effects were followed up with Bonferroni post-hocs. Relationships between the rates of change of metabolic and neuromuscular variables were assessed using Pearson's product-moment correlation coefficients. Statistical significance was set at $P<0.05$ and data are presented as mean ± SD.

RESULTS

The $\dot{V}O_2$peak measured in the ramp incremental test was 4.32 ± 0.46 L·min^{-1} (56 ± 8 mL·kg^{-1}·min^{-1}) and the peak work-rate was 385 ± 50 W. The GET occurred at 2.33 ± 0.34 L·min^{-1} and 137 ± 24 W.

Physiological responses within the severe-intensity domain

The T_{lim} in the severe-intensity CWR exercise tests ranged from 2.2 to 13.9 min. There were no differences between the three models (Equations 1-3) in the CP or W′ estimates ($P>0.05$; Table 1). The CP from the best fit model corresponded to 64 ± 7% of ramp test peak work-rate and 45 ± 11%Δ.

The $\dot{V}O_2$peak during the shorter (~85%Δ: 4.43 ± 0.50 L·min^{-1}), intermediate (~75%Δ: 4.49 ± 0.47 L·min^{-1}) and longer (~65%Δ: 4.41 ± 0.47 L·min^{-1}) severe-intensity tests were not different from the $\dot{V}O_2$peak achieved during the ramp incremental test (all P>0.05). Moreover, no significant differences were observed at T_{lim} among the three severe-intensity tests for any of the muscle tissue variables or for blood [lactate] (all P>0.05; Figure 2). There were also no differences in plasma [K^+] at T_{lim} among the shorter (5.6 ± 0.6 mM), intermediate (5.8 ± 1.1 mM,) and longer (5.7 ± 0.6 mM) severe-intensity tests (P>0.05).

Physiological responses during severe-, heavy- and moderate-intensity exercise

Pulmonary $\dot{V}O_2$, blood [lactate] and plasma [K^+] during moderate-, heavy- and severe-intensity exercise are illustrated in Figure 3**.** The T_{lim} for heavy-intensity exercise (231 ± 56 W) was 43.5 ± 16.2 min (range: 20.5 to 67.4 min) and the $\dot{V}O_2$ at T_{lim} (3.78 ± 0.53 L·min^{-1} ; 87 ± 4% of $\dot{V}O_2$peak) was lower than the ramp test $\dot{V}O_2$peak (P<0.05). The T_{lim} for the moderate-intensity exercise (113 ± 19 W) was 211.1 ± 57.0 min (range: 180 to 360 min) and the $\dot{V}O_2$ at T_{lim} (2.22 ± 0.38 L·min^{-1}, 52 ± 8% of $\dot{V}O_2$peak) was not different from the GET (P>0.05). In 9 out of 11 subjects the $\dot{V}O_2$ remained below the GET throughout the moderate exercise bout.

During severe-intensity exercise, blood [lactate] increased rapidly until T_{lim} and was significantly greater than baseline after 3 min (P<0.05). During heavy-intensity exercise, the rate of blood [lactate] increase was slower than during severe-intensity exercise such that blood [lactate] did not differ from baseline until after 10 min (P<0.05), and no further increase was observed between 10 min and T_{lim} (P>0.05) (Figure 3B). Plasma [K^+] was elevated above baseline at all measurement time points during heavy- and severe-intensity exercise (all P<0.05). The [K^+] continued to rise throughout severe-intensity exercise,

whereas it stabilised during heavy-intensity exercise beyond 6 min (Figure 3C). During moderate-intensity exercise, blood [lactate] did not change from baseline (P>0.05) while plasma [K^+] was elevated above resting baseline at 1 min (P<0.05), with no further increase thereafter (all time points P>0.05).

Muscle metabolic variables at rest and at T_{lim} following moderate-, heavy- and severe-intensity exercise are illustrated in Figure 4. For severe- and heavy-intensity exercise, muscle [ATP], [PCr] and pH were lower and muscle [lactate] was greater at T_{lim} relative to rest (all P<0.05). There was no significant muscle [glycogen] depletion during severe-intensity exercise relative to rest (P>0.05) but there was a tendency for glycogen depletion during heavy-intensity exercise (P=0.06). In contrast, for moderate-intensity exercise, muscle [PCr] at T_{lim} was greater than for severe- and heavy-intensity exercise (all P<0.05), and muscle [glycogen] was both lower than at rest and lower than at T_{lim} for heavy- and severe-intensity exercise (all P<0.05). Muscle [pH] and [lactate] did not change significantly from rest during moderate-intensity exercise (P>0.05).

Neuromuscular responses during severe-, heavy- and moderate-intensity exercise

The coefficients of variation (CV%) between trials during unloaded cycling were 25% (VL) and 35% (VM) for the peak-to-peak M-wave amplitude, and 32% (VL) and 32% (VM) for the M-wave total area. The CV% between stimulations during unloaded cycling was 11% (VL) and 9% (VM) for the peak-to-peak M-wave amplitude and 10% (VL) and 9% (VM) for the M-wave total area. The mean M_{max} amplitudes measured during cycling at 20 W below GET (VL 2.77 ± 1.43 and VM 0.99±1.18 mV) were not different between visits (all P>0.05). No significant differences were observed between trials in the neural drive to VL and VM during cycling at 20 W below GET.

Neuromuscular excitability: M-wave amplitude and M-wave area

The M-wave characteristics at T_{lim} for the three severe-intensity exercise tests, and for moderate-intensity, heavy-intensity and the mean of the severe-intensity exercise tests are shown in Figure 5A-D. Peripheral neuromuscular excitability at T_{lim}, indicated by the M-wave amplitude and M-wave area, did not differ among the severe-intensity tests (all $P<0.05$) (Figure 5A, C). The M-wave amplitude and M-wave area at T_{lim} were greater for severe-intensity exercise compared to both heavy- and moderate-intensity exercise in the VM ($P<0.05$), and the M-wave area at T_{lim} was also greater in severe- than in heavy-intensity exercise in VL ($P<0.05$) (Figure 5B, D). Differences in M-wave characteristics between severe-, heavy- and moderate-intensity exercise at each measurement time point are shown in Figure 6A-D.

Voluntary activation and neural drive

Voluntary muscle activation level, measured as EMG RMS amplitude, and neural drive, as indicated by RMS/M-wave amplitude, did not differ at T_{lim} among the severe-intensity exercise tests (all $P<0.05$) (Figure 5E, G). Both EMG RMS and RMS/M were greater at T_{lim} for severe-intensity compared to heavy- and moderate-intensity exercise in the VM ($P<0.05$) (Figure 5F). In the VL, the EMG RMS at T_{lim} was also greater for severe- than for heavy-intensity exercise and the RMS/M was greater for severe- than for moderate-intensity exercise (both $P<0.05$) (Figure 5F, H). The only difference in neuromuscular variables observed at T_{lim} between moderate- and heavy-intensity exercise was a significantly greater EMG RMS in the VL (Figure 5F). Differences in EMG RMS and RMS/M severe-, heavy- and moderate-intensity exercise at each measurement time point are shown in Figure 6E-H.

Relationships between physiological and neuromuscular variables

During severe-intensity exercise, the M-wave amplitude decreased in parallel with [PCr] depletion and plasma K^+ accumulation (Table 2). Moreover, increased neural drive (RMS/M) was correlated with high blood [lactate] and plasma [K^+], and to low muscle [PCr], and high muscle [lactate] and [glycogen] (Table 2). During heavy-intensity exercise, the reduction in M-wave amplitude was related to low muscle [PCr] and high plasma [K^+], and increased neural drive was related to high plasma [K^+] and low muscle [PCr], and high muscle [lactate] and [glycogen] (Table 2). During moderate-intensity exercise, the M-wave amplitude was inversely correlated with the reduction in [PCr] (Table 2).

DISCUSSION

To our knowledge, the present study is the first to combine muscle biopsy, blood analyses and measurements of neuromuscular excitability and neural drive (via electrical stimulation of the femoral nerve during exercise) to assess the muscle metabolic, acid-base and neuromuscular responses to cycling performed within discrete exercise intensity domains (32). The data presented herein provide novel insight into the *in vivo* relationships between exercise intensity, muscle metabolic perturbation and neuromuscular function and support the notion that LT/GET and CP separate exercise intensity domains within which exercise tolerance is limited by discrete fatigue mechanisms. In classical terms, when exercise intensity exceeds CP, the oxidation of fat and carbohydrate cannot keep pace with required ATP turnover and the rate of pyruvate production from glycolysis exceeds the capacity of the Krebs cycle, resulting in progressive increase in intramuscular lactate and H^+ concentrations. We demonstrated that a similar muscle metabolic milieu (i.e., [ATP], [PCr], [lactate] and pH) was attained at T_{lim} irrespective of work-rate within the severe-intensity domain. The muscle

metabolic perturbation was greater (i.e., lower [ATP] and pH, and higher [lactate]) at T_{lim} following severe- compared to heavy-intensity exercise, and also following severe- and heavy- compared to moderate-intensity exercise. In contrast, more extensive muscle glycogen depletion occurred during moderate- compared to both severe- and heavy-intensity exercise.

However, while the results indicate that CP represents a critical threshold for both muscle metabolic control and neuromuscular fatigue development, the importance of the GET in separating exercise intensity domains was less obvious; unlike some muscle metabolic, pulmonary gas exchange and blood [lactate] responses, neuromuscular indices of fatigue development were not strikingly different between moderate-intensity and heavy-intensity exercise.

Fatigue during severe-intensity exercise

The T_{lim} during the severe-intensity exercise tests ranged from 2.2 min to 13.9 min and in all cases, subjects achieved $\dot{V}O_2$peak. Historically, the amount of work that can be done above CP (i.e., the curvature constant of the power-duration relationship, W′), and therefore the cause(s) of exercise intolerance within the severe-intensity domain, has been linked to the depletion of the high-energy phosphates and a source related to anaerobic glycolysis, along with a finite amount of stored O_2 (43,44). Consistent with this, recent studies have demonstrated that, at least for small muscle mass exercise, the utilisation of this finite energy store (W′) coincides with the depletion of muscle PCr and the accumulation of fatigue-related metabolites (i.e. P_i, H^+) until a consistent, presumably 'limiting' value is attained (33, 69). The findings of the current study indicate that, irrespective of work-rate or exercise duration (~2-14 min), T_{lim} during severe-intensity exercise is associated with the attainment of consistently low values of muscle [PCr] (~23% of resting value), [ATP] (~76% of resting

483 value) and pH (~6.56), and consistently high values of muscle [lactate] (~1382% of resting
484 value), as well as blood [lactate] (~838% of resting value). It should be noted that the
485 observed muscle metabolite and substrate changes are reflective of the homogenate muscle
486 sample and therefore reflect the mean values for that particular muscle portion. It is known
487 that the depletion of muscle [PCr] during exercise displays significant regional heterogeneity
488 (13, 54). It is therefore possible that the subjects' eventual failure to maintain the requisite
489 power output was caused by the attainment of sufficiently low values of [PCr] and, perhaps,
490 [ATP], and/or sufficiently high values of muscle metabolites ($[P_i]$, [ADP], $[H^+]$ and their
491 sequelae) within some of the recruited muscle fibres (51; see also 3,23, 24). Clearly, subjects
492 either could not, or would not, tolerate this 'critical combination' of substrate and metabolite
493 concentrations, but it is not possible to ascertain whether this was related to direct effects of
494 the muscle metabolic milieu on contractile function (17) or to the attainment of some
495 individual sensory 'critical fatigue threshold' which might constrain central motor drive and
496 muscle activation via feedback from type III/IV neural afferents (4). The appreciable
497 metabolic perturbation we observed during severe-intensity exercise was associated with a
498 concomitant decrease in M-wave amplitude in both the VL and VM. A strong inverse
499 correlation was observed between both the voluntary EMG RMS amplitude and neural drive,
500 and the changes in [ATP] and [PCr] (Table 2). This is consistent with there being greater
501 engagement of central neural mechanisms (e.g. muscle fibre recruitment and firing frequency
502 modulation) in order to compensate for peripheral fatigue development.
503
504 We have proposed that the changes in muscle metabolic status that occur concomitantly with
505 the expenditure of the W′ are driving the development of the $\dot{V}O_2$ slow component during
506 severe-intensity exercise (8, 33, 70). Thus, exercise intolerance in this intensity domain is
507 associated with the complete utilisation of W′, the attainment of some 'critical' combination

of muscle substrate and/or metabolite concentrations, and the achievement of $\dot{V}_{O_2}$peak (8, 14, 47, 70). In the present study, we observed a reduction in muscle excitability in parallel with the increased metabolic stress. The reduction in muscle membrane excitability is likely mediated, at least in part, by changes in plasma [K^+] (Table 2), which may reflect a rise in interstitial [K^+] within the t-tubule weakening propagation of the action potential along the surface membrane. Increased extracellular [K^+] impairs force generation due to depolarisation of the cell membrane, resulting in a reduced amplitude of the action potential (11, 40). This process attenuates Ca^{2+} release from the sarcoplasmic reticulum, reducing cross-bridge formation and the force generating capacity of the myocyte (36). In our study, the increased plasma [K^+] was accompanied by a transient increase in neural drive which was brought about via a preservation of the EMG amplitude with reduced M-wave amplitude. It was notable that the reductions in M-wave amplitude and M-wave area in the VM during exhaustive severe exercise were less pronounced compared to moderate and heavy exercise (Figure 5 B and D), suggesting that the muscle excitability was preserved to a greater extent than at lower exercise intensities. It is important, however, to consider this finding in the context of increasing neural drive during severe exercise (Figure 6 G and H) which implies that exercise cessation was not due to central fatigue. Low muscle pH attained during severe exercise may attenuate the reduction in muscle membrane excitability (3, 24). Furthermore, the muscle glycogen content, a key regulator of sarcoplasmic Ca^{2+} release rate and thus muscle excitability (15, 50), did not fall significantly during severe exercise. Precisely how the utilisation of the W′, the associated alterations in muscle substrate and metabolite concentrations, and ionic changes influence muscle excitability warrants further investigation.

Fatigue during heavy-intensity exercise

Heavy-intensity exercise was maintained for an average of 43.5 min (T_{lim} ranged from 20.5 to 67.4 min) and, in contrast to severe-intensity exercise, no subject achieved $\dot{V}_{O_2}$peak at T_{lim} (~87% $\dot{V}_{O_2}$peak). Consistent with our second hypothesis, the muscle metabolic perturbation experienced following heavy-intensity exercise was less than that observed following severe-intensity exercise, but was greater than that observed following moderate-intensity exercise. At T_{lim}, significant reductions were observed in muscle [PCr] (~66%), [ATP] (~12%), [pH] (~97%]) and [glycogen] (~59%), and there was a significant increase in muscle [lactate] (~447%) relative to resting values. Similarly, blood [lactate] and plasma [K^+] displayed greater perturbation relative to moderate-intensity exercise, but less perturbation relative to severe-intensity exercise (Figure 3). It is of interest that the decrease in muscle excitability from rest to T_{lim} was greater during heavy-intensity than during severe-intensity exercise (Figure 5). Following the onset of exercise, plasma [K^+] increased rapidly to attain a peak value at 10 min which was sustained until T_{lim}; the reduction in M-wave amplitude followed a similar temporal profile. It is therefore likely that the initial reduction in M-wave amplitude was a result of plasma [K^+] accumulation which reduced the release of Ca^{2+} from the sarcoplasmic reticulum, impairing excitation-contraction coupling (36, 71). As heavy-intensity exercise continued, it is possible that the combined metabolic and ionic perturbation, coupled with the ~60% decrease in muscle [glycogen], may have further impaired Ca^{2+} release and cross-bridge formation (2, 3, 23, 24, 36, 40, 41) and/or the sensitivity of the myofilaments to Ca^{2+} (17). Although more complicated than for severe-intensity exercise, fatigue development during heavy-intensity exercise appears to be related to the combined influence of ionic changes on muscle membrane excitability, muscle metabolite accumulation, and the decrease in energy substrate, which act collectively to impair excitation-contraction coupling.

Fatigue during moderate-intensity exercise

Moderate-intensity exercise, performed at a work-rate of 20 W below the GET, was continued for an average of 211 min with subjects working at ~52% $\dot{V}O_2$peak at T_{lim}. Muscle metabolic perturbation was relatively slight in this domain (Figure 3). For example, at the end of exercise, muscle [PCr] had fallen to ~76% of the baseline value and pH had fallen by 0.1 unit from the resting value, while blood [lactate] and plasma [K^+] were also largely unchanged (Figures 3 and 4). There was, however, a large reduction (–83%) in muscle [glycogen] (1, 29, 59, 60). It is therefore likely that the development of peripheral fatigue within the moderate-intensity domain is related to the depletion of muscle glycogen and impairment in neuromuscular excitability and transmission (15, 28, 49, 50, 62). In addition to being an essential substrate for the regeneration of ATP, it has been demonstrated that under conditions where [ATP] is held high, that low muscle [glycogen] can impair muscle function (49, 62). The association between low muscle [glycogen] and impaired muscle function can be attributed to glycogen's modulatory role in the release of Ca^{2+} from the sarcoplasmic reticulum (15, 19, 20, 28, 49, 50). In keeping with glycogen's role in excitation-contraction coupling, individuals deficient in glycogen phosphorylase (McArdle's disease) do not experience a considerable fall in pH but demonstrate an earlier decline in the M-wave amplitude during exercise (16). Furthermore, glucose administration during exercise has been shown to partially restore both the M-wave amplitude and muscle contractility (34, 37, 63) supporting the notion that carbohydrate availability modulates muscle excitability and contractile function. The findings of the present study show that moderate-intensity exercise (<GET) can be sustained for a long duration with little change in muscle metabolites and indicate that muscle glycogen depletion is the likely mechanism responsible for the decline in neuromuscular function and exercise intolerance in this domain.

583 The majority of research investigating neuromuscular fatigue development during exercise
584 has focused on small muscle groups and has been limited to the assessment of neuromuscular
585 function pre-exercise and as soon as possible (usually within 2-3 minutes) post-exercise.
586 Considering the task-specific nature of neuromuscular fatigue development, and the rapid
587 recovery in muscle function (within 2 min) after high-intensity cycle exercise (26), it is
588 possible that the previously reported changes in neuromuscular function pre- to post-exercise
589 underestimate fatigue development *during* exercise. Recently, Sidhu et al. (56) adopted an
590 approach that uses the motor compound action potential (M-wave) for the assessment of
591 changes in neuromuscular function during cycle exercise. Adopting a similar approach to
592 Sidhu et al. (56), we found large reductions in the M-wave amplitude and M-wave area in
593 both the VL and VM during exercise to T_{lim} in each discrete exercise intensity domain. This
594 suggests that changes in muscle excitability linked to the fatigue process can occur
595 consequent to a wide range of perturbations in muscle and blood chemistry, with limited
596 differentiation between exercise intensity domains. The consistency of indices of
597 neuromuscular fatigue during severe-intensity cycling exercise in our study contrasts with a
598 recent report of Thomas et al. (65) in which peripheral fatigue, assessed post-exercise using
599 electrical stimulation during isometric contractions, was greater at higher work-rates within
600 the severe-intensity domain. It is possible that this reflects differences in the experimental
601 techniques employed, and underlines the importance of accounting for the task-specificity of
602 fatigue and the dynamics of muscle recovery post-exercise (10).
603
604 **Conclusion**
605 This study employed a novel and rather comprehensive combination of invasive and non-
606 invasive techniques that enabled simultaneous assessment of metabolic, ionic, systemic and
607 neuromuscular factors that define muscular performance. Although direct measures of the

608 contribution of central factors to fatigue were not employed, peripheral nerve stimulation permitted
609 elucidation of their relative importance in neuromuscular fatigue development during
610 exhaustive cycle exercise performed within each of the well-defined exercise intensity
611 domains. This study is consistent with the notion that the GET and the CP demarcate exercise
612 intensity domains within which fatigue is mediated by distinct mechanisms. Exercise
613 intolerance within the severe-intensity domain (>CP) was associated with the attainment of a
614 consistent critical muscle metabolic milieu (i.e., low [PCr] and pH and high [P_i]). In contrast,
615 moderate-intensity exercise (<GET) was associated with more significant depletion of muscle
616 [glycogen]. The cause(s) of fatigue during heavy-intensity exercise (>GET, <CP) was/were
617 more obscure with intermediate changes in muscle metabolic perturbation and glycogen
618 depletion being apparent. These results are consistent with the notion that both the GET and
619 CP demarcate exercise intensity domains characterised by distinct respiratory and metabolic
620 profiles. Strikingly, CP represents a boundary above which both metabolic and
621 neuromuscular responses conform to a consistent ceiling or nadir irrespective of work-rate
622 and exercise duration.
623

REFERENCES

1. Ahlborg B, Bergstrom J, Ekelund LG, Hultman E. Muscle glycogen and muscle electrolytes during prolonged physical exercise. *Acta Physiol Scand* 70: 129-42, 1967.

2. Allen DG. Fatigue in working muscles. *J Appl Physiol* 106: 358-9, 2009.

3. Allen DG, Lamb GD, Westerblad H. Skeletal muscle fatigue: Cellular mechanisms. *Physiol Rev* 88: 287-332, 2008.

4. Amann M, Dempsey JA. Ensemble input of group III/IV muscle afferents to CNS: a limiting factor of central motor drive during endurance exercise from normoxia to moderate hypoxia. *Adv Exp Med Biol* 903: 325-42. 2016.

5. Beaver WL, Wasserman K, Whipp BJ. A new method for detecting anaerobic threshold by gas exchange. *J Appl Physiol* 60: 2020-7, 1986.

6. Bergstrom J. Percutaneous needle biopsy of skeletal muscle in physiological and clinical research. *Scand J Clin Lab Invest* 35: 609-16, 1975.

7. Black MI, Jones AM, Bailey SJ, Vanhatalo A. Self-pacing increases critical power and improves performance during severe-intensity exercise. *Appl Physiol Nutr Metab* 40: 662-70, 2015.

8. Burnley M, Jones AM. Oxygen uptake kinetics as a determinant of sports performance. *Eur J Sport Sci 7*: 63-79, 2007.

9. Burnley M, Vanhatalo A, Fulford J, Jones AM. Similar metabolic perturbations during all-out and constant force exhaustive exercise in humans: a ^{31}P magnetic resonance spectroscopy study. *Exp Physiol* 95: 798-807, 2010.

10. Burnley, M. Vanhatalo A, Jones AM. Distinct profiles of neuromuscular fatigue during muscle contractions below and above the critical torque in humans. *J Appl Physiol* 113: 215-23, 2012.

11. Cairns SP, Hing WA, Slack JR, Mills RG, Loiselle DS. Different effects of raised [K+]o on membrane potential and contraction in mouse fast- and slow-twitch muscle. *Am J Physiol* 273: C598-611, 1997.

12. Calbet JAL, Jensen-Urstad M, van Hall G, Homberg HC, Rosdahl H, Saltin B. Maximal muscular vascular conductances during whole body upright exercise in humans. *J Physiol* 558: 319-31, 2004.

13. Cannon DT, Howe FA, Whipp BJ, Ward SA, McIntyre DJ, Ladroue C, Griffiths JR, Kemp GJ, Rossiter HB. Muscle metabolism and activation heterogeneity by combined ^{31}P chemical shift and T2 imaging, and pulmonary O_2 uptake during incremental knee-extensor exercise. *J Appl Physiol* 115: 839-49, 2013.

14. Chidnok W, Fulford J, Bailey SJ, DiMenna FJ, Skiba PF, Vanhatalo A, Jones AM. Muscle metabolic determinants of exercise tolerance following exhaustion: relationship to the "critical power". *J Appl Physiol* 115: 243-50, 2013.

15. Chin ER, Allen DG. Effects of reduced muscle glycogen concentration on force, Ca2+ release and contractile protein function in intact mouse skeletal muscle. *J Physiol* 498: 17-29, 1997.

16. Cooper RG, Stokes MJ, Edwards RH. Myofibrillar activation failure in McArdle's disease. *J Neurol Sci* 1: 1-10. 1989.

17. Debold EP, Fitts RH, Sundberg CW, Nosek TM. Muscle fatigue from the perspective of a single cross-bridge. *Med Sci Sports Exerc* In press. DOI:10.1249/MSS.0000000000001047, 2016.

18. De Luca CJ. The use of surface electromyography in biomechanics. *J Appl Biomech* 13: 135-63. 1993.

19. Duhamel TA, Green HJ, Perco JG, Ouyang J. Effects of prior exercise and a low-carbohydrate diet on muscle sarcoplasmic reticulum function during cycling in women. *J Appl Physiol* 101: 695-706, 2006a.

20. Duhamel TA, Perco JG, Green HJ. Manipulation of dietary carbohydrates after prolonged effort modifies muscle sarcoplasmic reticulum responses in exercising males. *Am J Physiol Reg Int Comp Physiol* 291: R1100-10, 2006b.

21. Enoka RM, Ducheateau. Muscle fatigue: what, why and how it influences muscle function. *J Physiol* 586: 11-23, 2008.

22. Enoka RM, Stuart DG. Neurobiology of muscle fatigue. *J Appl Physiol* 72: 1631-48, 1992.

23. Fitts RH. Cellular mechanisms of muscle fatigue. *Physiol Rev* 74: 49-94, 1994.

24. Fitts RH. The cross-bridge cycle and skeletal muscle fatigue. *J Appl Physiol* 104: 551-8, 2008.

25. Fowles JR, Green HJ, Tupling R, O'Brien S, Roy BD. Human neuromuscular fatigue is associated with altered Na+-K+-ATPase activity following isometric exercise. *J Appl Physiol* 92: 1585-93, 2002.

26. Froyd C, Millet GY, Noakes TD. The development of peripheral fatigue and short-term recovery during self-paced high-intensity exercise. *J Physiol* 591: 1339-46. 2013.

27. Gandevia SC. Spinal and supraspinal factors in human muscle fatigue. *Physiol Rev* 81: 1725-89, 2001.

28. Gejl KD, Hvid LG, Frandsen U, Jensen K, Sahlin K, Ortenblad N. Muscle glycogen content modifies SR Ca^{2+} release rate in elite endurance athletes. *Med Sci Sports Exerc* 46: 496-505, 2014.

29. Gollnick PD, Piehl K, Saltin B. Selective glycogen depletion pattern in human muscle fibres after exercise of varying intensity and varying pedalling rates. *J Physiol* 241: 45-57, 1974.

30. Green HJ. Cation pumps in skeletal muscle: potential role in muscle fatigue. *Acta Physiol Scand* 162: 201-13, 1998.

31. Hogan MC, Richardson RS, Haseler LJ. Human muscle performance and PCr hydrolysis with varied oxygen fractions: a ^{31}P-MRS study. *J Appl Physiol* 86: 1367-73, 1999.

32. Jones AM, Poole DC. Introduction to oxygen uptake kinetics and historical development of the discipline. In AM Jones and DC Poole (Eds), Oxygen uptake kinetics in sport, exercise and medicine (pp 2-35). London and New York, NY: Routledge, 2005.

33. Jones AM, Wilkerson DP, DiMenna F, Fulford J, Poole DC. Muscle metabolic responses to exercise above and below the "critical power" assessed using ^{31}P-MRS. *Am J Physiol Regul Integr Comp Physiol* 294: R585-93, 2008.

34. Karelis AD, Peronnet F, Gardiner PF. Glucose infusion attenuates muscle fatigue in rat plantaris muscle during prolonged indirect stimulation in situ. *Exp Physiol* 87: 585-92, 2002.

748 35. Lowry OH, Passonneau JV. A flexible system of enzymatic analysis. Academic Press,
749 New York, 1972.
750
751 36. MacIntosh BR, Holash RJ, Renaud JM. Skeletal muscle fatigue – regulation of
752 excitation-contraction coupling to avoid metabolic catastrophe. *J Cell Sci* 125: 2105-
753 14, 2012.
754
755 37. Marcil M, Karelis AD, Peronnet F, Gardiner PF. Glucose infusion attenuates fatigue
756 without sparing glycogen in rat soleus muscle during prolonged electrical stimulation
757 in situ. *Eur J Appl Physiol* 93: 569-74. 2005.
758
759 38. Martin V, Kerherve H, Messonnier LA, Banfi JC, Geyssant A, Bonnefoy R, Feasson
760 L, Millet GY. Central and peripheral contributions to neuromuscular fatigue induced
761 by a 24-h treadmill run. *J Appl Physiol* 108: 1224-33, 2010.
762
763 39. Matkowski B, Place N, Martin A, Lepers R. Neuromuscular fatigue differs following
764 unilateral vs bilateral sustained submaximal contractions. *Scand J Med Sci Sports* 21:
765 268-76, 2011.
766
767 40. McKenna MJ. The roles of ionic processes in muscular fatigue during intense
768 exercise. *Sports Med* 13: 134-45, 1992.
769
770 41. McKenna MJ, Bangsbo J, Renaud JM. Muscle K^+, Na^+ and Cl^- disturbances and Na^+-
771 K^+ pump inactivation: implications for fatigue. *J Appl Physiol* 104: 288-95, 2008.
772

42. Millet GY, Lepers R. Alterations of neuromuscular function after prolonged running, cycling and skiing exercises. *Sports Med* 34: 105-16, 2004.

43. Monod H, Scherrer J. The work capacity of a synergic muscle group. *Ergonomics* 8: 329-38, 1965.

44. Moritani T, Nagata A, deVries HA, Muro M. Critical power as a measure of physical work capacity and anaerobic threshold. *Ergonomics* 24: 339-50, 1981.

45. Morris MG, Dawes H, Howells K, Scott OM, Cramp M, Izadi H. Alterations in peripheral muscle contractile characteristics following high and low intensity bouts of exercise. *Eur J Appl Physiol* 112: 337-43, 2012.

46. Mortensen SP, Damsgaard R, Dawson EA, Secher NH, Gonzalez-Alonso J. Restrictions in systemic and locomotor skeletal muscle perfusion, oxygen supply and VO_2 during high-intensity whole-body exercise in humans. *J Physiol* 586: 2621-35, 2008.

47. Murgatroyd SR, Ferguson C, Ward SA, Whipp BJ, Rossiter HB. Pulmonary O2 uptake kinetics as a determinant of high-intensity exercise tolerance in humans. *J Appl Physiol* (1985) 110:1598-606, 2011.

48. Newham DJ, Cady EB. A ^{31}P study of fatigue and metabolism in human skeletal muscle with voluntary, intermittent contractions at different forces. *NMR Biomed* 3: 211-19, 1990.

49. Nielsen J, Schroder HD, Rix CG, Ortenblad N. Distinct effects of subcellular glycogen localization on tetanic relaxation time and endurance in mechanically skinned rat skeletal muscle fibres. *J Physiol* 587: 3679-90, 2009.

50. Ortenblad N, Nielsen J, Saltin B, Holmberg HC. Role of glycogen availability in sarcoplasmic reticulum Ca^{2+} kinetics in human skeletal muscle. *J Physiol* 589: 711-25, 2011.

51. Poole DC, Ward SA, Gardner GW, Whipp BJ. Metabolic and respiratory profile of the upper limit for prolonged exercise in man. *Ergonomics* 31: 1265-79, 1988.

52. Rossman MJ, Garten RS, Venturelli M, Amann M, Richardson RS. The role of active muscle mass in determining the magnitude of peripheral fatigue during dynamic exercise. *Am J Physiol Regul Integr Comp Physiol* 306: R934-40, 2014.

53. Rossman MJ, Venturelli M, McDaniel J, Amann M, Richardson RS. Muscle mass and peripheral fatigue: a potential role for afferent feedback? *Acta Physiol* 206: 242-50, 2012.

54. Sahlin K, Söderlund K, Tonkonogi M, Hirakoba K. Phosphocreatine content in single fibers of human muscle after sustained submaximal exercise. *Am J Cell Physiol* 273: C172-8, 1997.

55. Sejersted OM, Sjøgaard G. Dynamics and consequences of potassium shifts in skeletal muscle and heart during exercise. *Physiol Rev* 80: 1411-81, 2000.

56. Sidhu SK, Cresswell AG, Carroll TJ. Motor cortex excitability does not increase during sustained cycling exercise to volitional exhaustion. J Appl Physiol (1985). 113:401-9, 2012.

57. Smith JL, Martin PG, Gandevia SC, Taylor JL. Sustained contraction at very low forces produces prominent supraspinal fatigue in human elbow flexor muscles. *J Appl Physiol* 103: 560-8, 2007.

58. Smith JR, Ade CJ, Broxterman RM, Skutnik BC, Barstow TJ. Influence of exercise intensity on respiratory muscle fatigue and brachial artery blood flow during cycling exercise. *Eur J Appl Physiol* 114: 1767-77, 2014.

59. Sjøgaard G. Electrolytes in slow and fast muscle fibers of humans at rest and with dynamic exercise. *Am J Physiol Regul Integr Comp Physiol* 245: R25-31, 1983.

60. Sjøgaard G. Water and electrolyte fluxes during exercise and their relation to muscle fatigue. *Acta Physiol Scand Suppl* 556: 129-36, 1986.

61. Søgaard K, Gandevia SC, Todd G, Petersen NT, Taylor JL. The effect of sustained low-intensity contractions on supraspinal fatigue in human elbow flexor muscles. *J Physiol* 573: 511-23, 2006.

62. Stephenson DG, Nguyen LT, Stephenson GM. Glycogen content and excitation-contraction coupling in mechanically skinned muscle fibres of the cane toad. *J Physiol* 519: 177-187, 1999.

63. Stewart RD, Duhamel TA, Foley KP, Ouyang J, Smith IC, Green HJ. Protection of muscle membrane excitability during prolonged cycle exercise with glucose supplementation. *J Appl Physiol* 103: 331-9, 2007.

64. Tomazin K, Morin JB, Strojnik V, Podpecan A, Millet GY. Fatigue after short (100-m), medium (200-m) and long (400-m) treadmill sprints. *Eur J Appl Physiol* 112: 1027-36, 2012.

65. Thomas K, Elmeua M, Howatson G, Goodall S. Intensity-Dependent Contribution of Neuromuscular Fatigue after Constant-Load Cycling. *Med Sci Sports Exerc* 48:1751-60, 2016.

66. Thomas K, Goodall S, Stone M, Howatson G, St Clair Gibson A, Ansley L. Central and peripheral fatigue in male cyclists after 4, 20 and 40 km time trials. *Med Sci Sport Exerc* 47: 537-46, 2015.

67. Vanderthommen M, Duteil S, Wary C, Raynaud JS, Leroy-Willig A, Crielaard JM, Carlier PG. A comparison of voluntary and electrically induced contractions by interleaved 1 H- and 31P-NMRS in humans. *J Appl Physiol* 94: 1012-24, 2003.

68. Vanhatalo A, Black MI, DiMenna FJ, Blackwell JR, Schmidt JF, Thompson C, Wylie LJ, Mohr M, Bangsbo J, Krustrup P, Jones AM. The mechanistic bases of the power–time relationship: muscle metabolic responses and relationships to muscle fibre type. *J Physiol* 594: 4407-23, 2016.

69. Vanhatalo A, Fulford J, DiMenna F, Jones AM. Influence of hyperoxia on muscle metabolic responses and the power-duration relationship during severe-intensity exercise in humans: a ^{31}P magnetic resonance spectroscopy study. *Exp Physiol* 95: 528-40, 2010.

70. Vanhatalo A, Poole DC, DiMenna FJ, Bailey SJ, Jones AM. Muscle fiber recruitment and the slow component of O2 uptake: constant work rate vs. all-out sprint exercise. *Am J Physiol Regul Integr Comp Physiol* 300:R700-7, 2011.

71. Westerblad H, Allen DG. Cellular mechanisms of skeletal muscle fatigue. *Adv Exp Med Biol* 538: 563-70, 2003.

72. Whipp BJ, Ward SA. Pulmonary gas exchange dynamics and the tolerance to muscular exercise: effects of fitness and training. *Ann Physiol Anthropol* 11: 207-14, 1992.

73. Whipp BJ, Wasserman K. Oxygen uptake kinetics for various intensities of constant-load work. *J Appl Physiol* 33: 351-6, 1972.

74. Wuthrich TU, Eberle EC, Spengler CM. Locomotor and diaphragm muscle fatigue in endurance athletes performing time-trials of different durations. *Eur J Appl Physiol* 114: 1619-33, 2014.

899 **Figure Legends**

900

901 **Table 1** The CP and W′ parameter estimates derived from Equations 1-3 and the 'best fit'
902 model.

903

904 **Table 2** The correlation coefficients between the rate of change in blood and muscle tissue
905 variables and the rate of change in neuromuscular variables measured in *m. vastus lateralis*. *
906 $P<0.05$.

907

908 **Figure 1**. Schematic of the exercise protocol. Group mean work-rates are shown for the
909 severe- (solid line), heavy- (dotted line) and moderate- (dashed line) intensity trials. All trials
910 were started with a 3-min "warm-up" phase at 20 W, followed by an immediate "step"
911 increase to the required work-rate. Subjects were encouraged to continue exercising for as
912 long as possible. The dashed arrows indicate the collection of venous blood, and femoral
913 nerve stimulation. The solid arrows indicate the collection of muscle tissue. N.B., for clarity,
914 the resting muscle sample obtained prior to the first trial is not shown.

915 **Figure 2**. Muscle metabolic responses ([ATP] panel A, [PCr] panel B, pH panel C, [lactate]
916 panel D, [glycogen] panel E) and blood [lactate] (panel F) at T_{lim} were not different following
917 exhaustive exercise at three different severe-intensity work-rates. R = rest; S1 = short trials at
918 ~85%Δ (T_{lim} = 224 ± 41 s); S2 = intermediate trials at ~75%Δ (T_{lim} = 333 ± 131 s); and S3 =
919 long trials at ~65%Δ (T_{lim} = 475 ± 145 s). * Different from S1, S2 and S3 ($P<0.05$).

920 **Figure 3**. Pulmonary $\dot{V}O_2$ (panel A), blood [lactate], (panel B) and plasma [K^+] (panel C)
921 response to severe- (solid circle), heavy- (clear circle) and moderate- (solid triangle) intensity

922 exercise. To aid clarity error bars have been omitted from all but the final data point. a =
923 different from moderate-intensity $P<0.05$; b = different from heavy-intensity $P<0.05$.
924
925 **Figure 4.** Muscle [ATP] (panel A), [PCr] (panel B), [pH] (panel C), [lactate] (panel D), and
926 [glycogen] (panel E) at rest (white triangle), and following severe- (black circle), heavy-
927 (white circle), and moderate-intensity exercise (black triangle). * = different from rest
928 $P<0.05$; a = different from moderate-intensity $P<0.05$; b = different from heavy-intensity
929 $P<0.05$; c = different from severe-intensity $P<0.05$.
930
931 **Figure 5.** The group mean ± SD M-wave amplitude and M-wave area (normalised to
932 maximum M-wave during baseline pedalling) indicating peripheral neuromuscular
933 excitability (panels A-D); voluntary EMG RMS amplitude (normalised to M-wave amplitude
934 at 1 min of exercise) indicating muscle activation level (panels E and F); and RMS/M-wave
935 (normalised to corresponding M-wave amplitude at each measurement time point) indicating
936 central fatigue (panels G and H) at the limit of tolerance (T_{lim}) for moderate-, heavy- and
937 severe-intensity exercise (panels B, D, F, H) and for three work-rates (severe 1 ~85%Δ,
938 severe 2 ~75%Δ and severe 3 ~65%Δ) within the severe-intensity domain (panels A, C, E,
939 G). There were no significant differences among the severe-intensity work-rates in muscle
940 excitability (A, C) or in indices of central fatigue (E, G). VL = *m. vastus lateralis*; VM = *m.*
941 *vastus medialis*; EMG = electromyogram; RMS = root mean square; a = different from
942 moderate-intensity $P<0.05$; b = different from heavy-intensity $P<0.05$; c = different from
943 severe-intensity $P<0.05$.
944
945 **Figure 6.** The normalised M-wave amplitude (panels A and B), M-wave area (panels C and
946 D), voluntary EMG RMS amplitude (panels E and F), and RMS/M-wave amplitude (panels G

947 and H) during severe- (solid circle), heavy- (clear circle), and moderate-intensity (solid
948 triangle) exercise in *m. vastus lateralis* (VL) and *vastus medialis* (VM). M-wave amplitude
949 and area were normalised to maximum M-wave during baseline pedalling, EMG RMS was
950 normalised to M-wave amplitude at 1 min of exercise, and RMS/M-wave was normalised to
951 corresponding M-wave amplitude at each measurement time point. Error bars have been
952 omitted from all but the final data point to aid clarity. [a] Different from rest; [b] different from
953 severe-intensity ($P<0.05$); [c] different from heavy-intensity ($P<0.05$); [d] different from
954 moderate-intensity ($P<0.05$); and [e] trend for difference from heavy-intensity ($P=0.055$).
955
956

Table 1 The parameter estimates derived from Equations 1-3 and the 'optimised fit' model.

	R^2	CP (W)	SEE (W)	CV%	W' (kJ)	SEE (kJ)	CV%
W-Tlim model	0.993 – 1.000	253 ± 54	6 ± 3	2.6 ± 1.4	22.5 ± 5.3	2.3 ± 1.0	11.0 ± 6.2
1/Tlim model	0.939 – 0.999	252 ± 52	7 ± 4	3.0 ± 2.3	20.7 ± 5.2	1.9 ± 1.1	9.5 ± 5.6
P-Tlim model	0.919 – 1.000	248 ± 52	5 ± 3	2.2 ± 1.4	22.4 ± 3.8	2.5 ± 1.8	11.3 ± 9.4
Optimised fit model	0.944 – 1.000	250 ± 53	5 ± 2	2.0 ± 1.2	22.5 ± 6.1	1.8 ± 0.8	8.3 ± 4.5

Table 2. The correlation coefficients between the rate of change in blood and muscle tissue variables and the rate of change in neuromuscular variables measured in *m. vastus lateralis*. * $P<0.05$.

			M-wave Amplitude	Voluntary EMG	Neural Drive
Severe	n = 33	**BLa**	-0.30	0.57*	0.47*
		Plasma [K^+]	-0.39*	0.68*	0.64*
	n = 24	**[PCr]**	0.59*	-0.80*	-0.80*
		[lactate]	-0.40	0.44*	0.55*
		[glycogen]	-0.22	0.46*	0.56*
		[pH]	-0.13	0.36	0.37
		[ATP]	0.21	-0.60*	-0.59*
Heavy	n = 10	**BLa**	-0.42	0.13	0.49
		Plasma [K^+]	-0.88*	-0.29	0.86*
	n = 7	**[PCr]**	0.93*	-0.28	-0.72*
		[lactate]	-0.25	0.63	0.66
		[glycogen]	-0.15	0.53	0.77*
		[pH]	0.13	0.78*	0.27
		[ATP]	-0.26	0.32	0.63
Moderate	n = 10	**BLa**	0.08	0.05	0.10
		Plasma [K^+]	0.12	0.18	0.49
	n = 7	**[PCr]**	-0.67*	-0.36	0.58
		[lactate]	-0.44	-0.34	0.04
		[glycogen]	-0.10	0.43	0.23
		[pH]	0.19	0.06	-0.30
		[ATP]	0.09	0.59	0.24

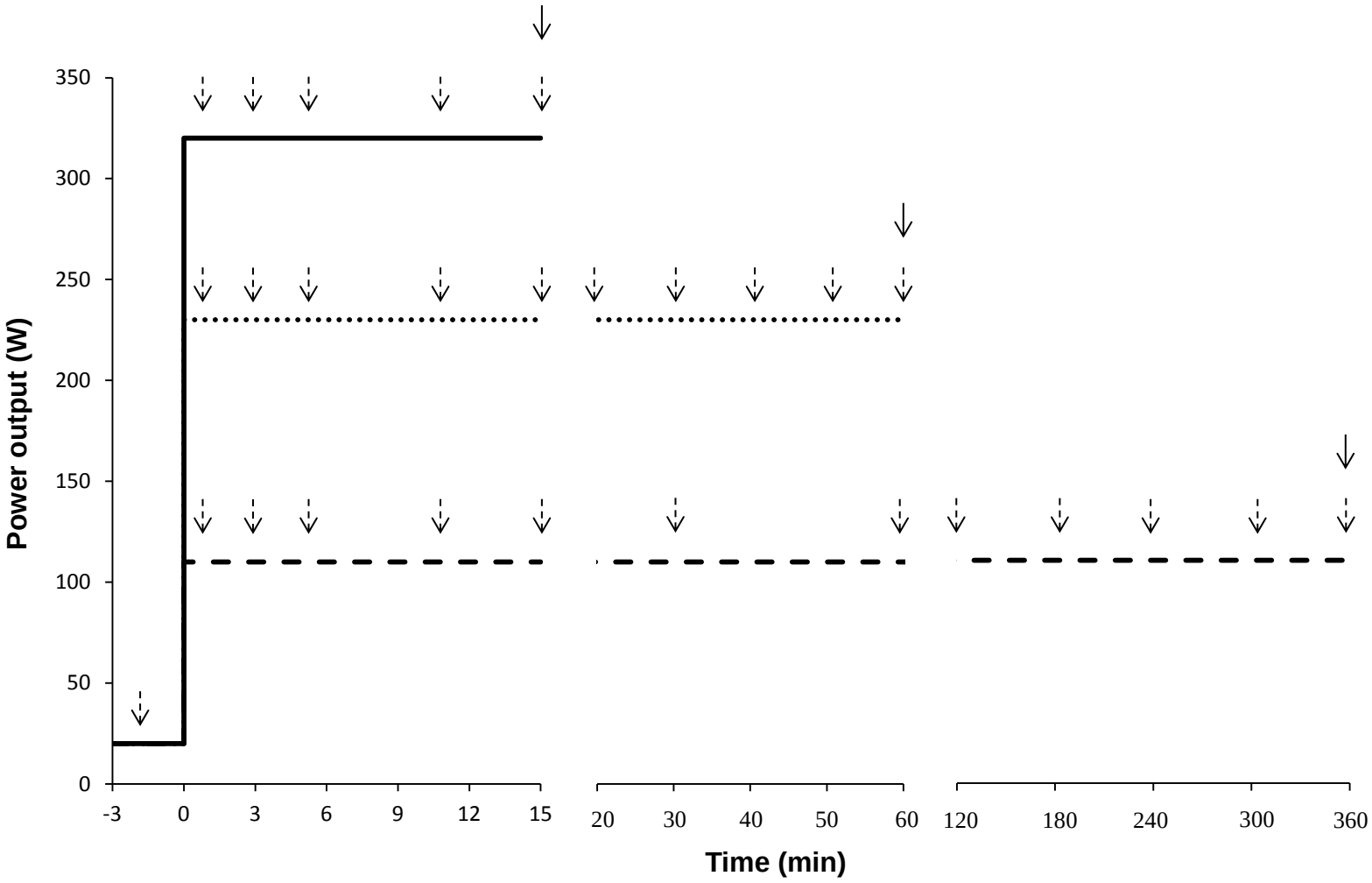
Power output (W)
350
300
250
200
150
100
50
0
-3
0
3
6
9
12
15
20
30
40
50
60
120
180
240
300
360
Time (min)

Figure 1

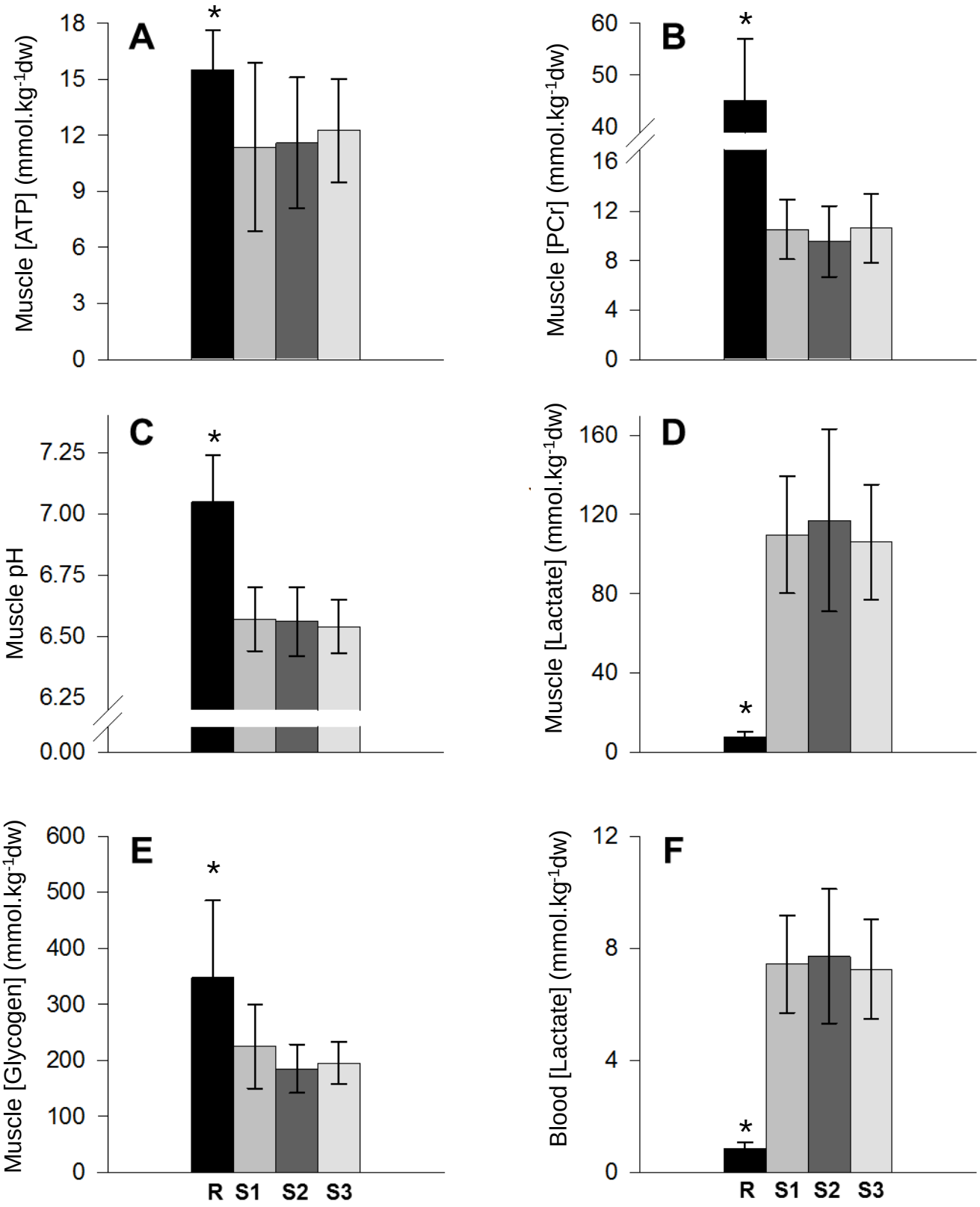
A
Muscle [ATP] (mmol.kg-1dw)
18
15
12
9
6
3
0
*
B
Muscle [PCr] (mmol.kg-1dw)
60
50
40
16
12
8
4
0
*
C
Muscle pH
7.25
7.00
6.75
6.50
6.25
0.00
*
D
Muscle [Lactate] (mmol.kg-1dw)
160
120
80
40
0
*
E
Muscle [Glycogen] (mmol.kg-1dw)
600
500
400
300
200
100
0
*
R S1 S2 S3
F
Blood [Lactate] (mmol.kg-1dw)
12
8
4
0
*
R S1 S2 S3

Figure 2

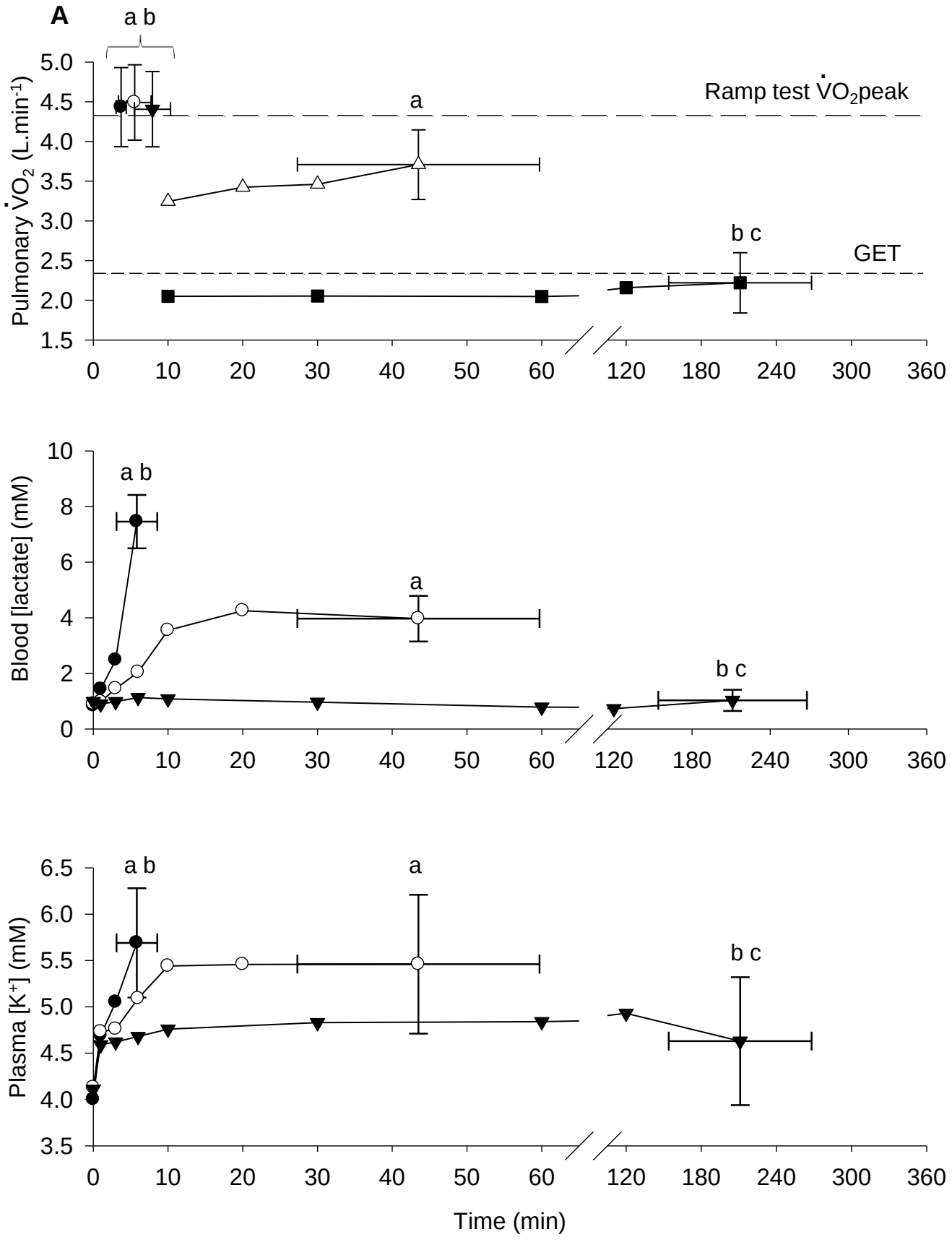
A
a b
a
b c
Ramp test V̇O2peak
GET
Pulmonary V̇O2 (L.min-1)
Blood [lactate] (mM)
Plasma [K+] (mM)
Time (min)

Figure 3

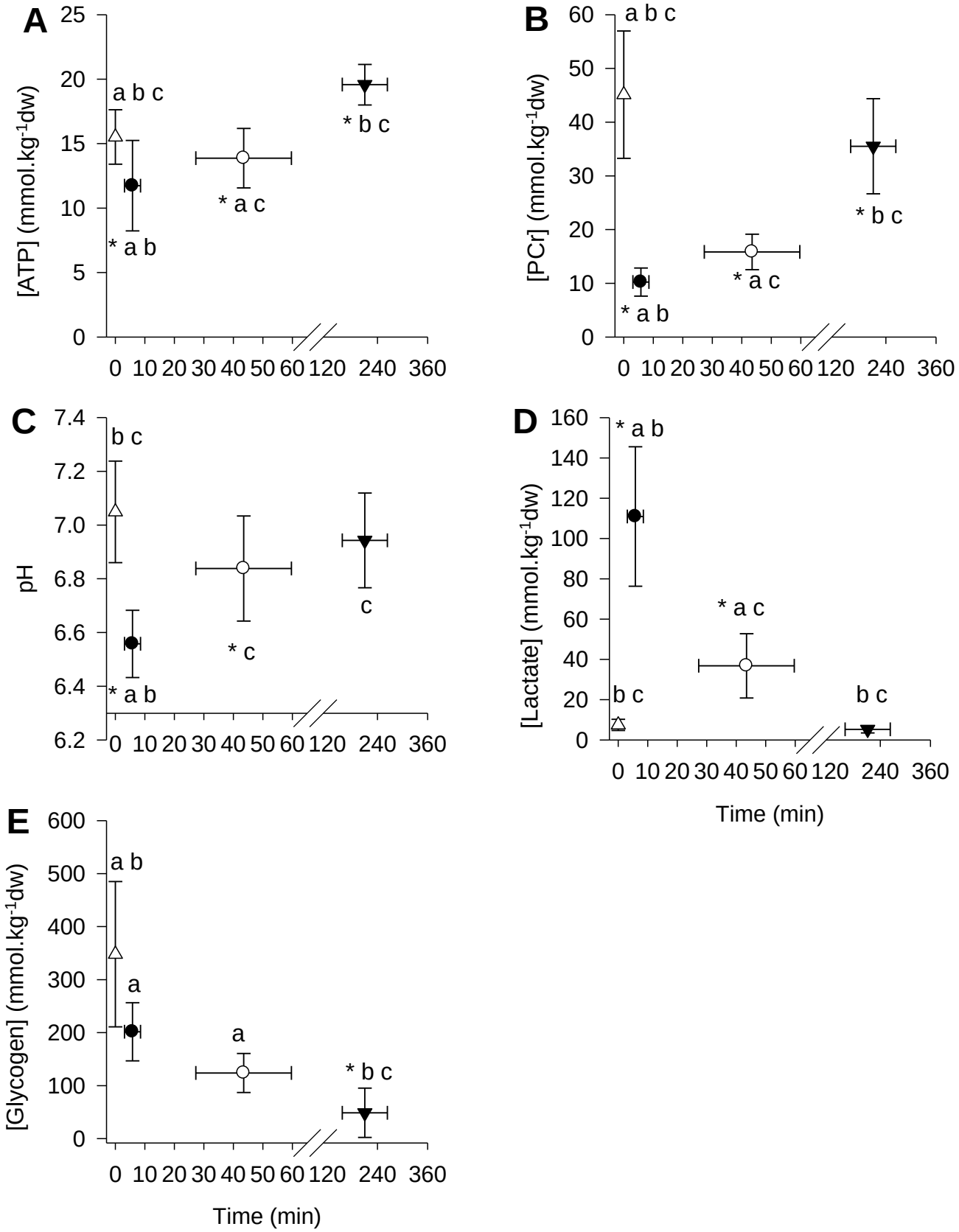
A
[ATP] (mmol.kg-1dw)
25
20
15
10
5
0
a b c
* a b
* a c
* b c
0 10 20 30 40 50 60 120 240 360
B
[PCr] (mmol.kg-1dw)
60
50
40
30
20
10
0
a b c
* a b
* a c
* b c
0 10 20 30 40 50 60 120 240 360
C
pH
7.4
7.2
7.0
6.8
6.6
6.4
6.2
b c
* a b
* c
c
0 10 20 30 40 50 60 120 240 360
D
[Lactate] (mmol.kg-1dw)
160
140
120
100
80
60
40
20
0
* a b
b c
* a c
b c
0 10 20 30 40 50 60 120 240 360
Time (min)
E
[Glycogen] (mmol.kg-1dw)
600
500
400
300
200
100
0
a b
a
a
* b c
0 10 20 30 40 50 60 120 240 360
Time (min)

Figure 4

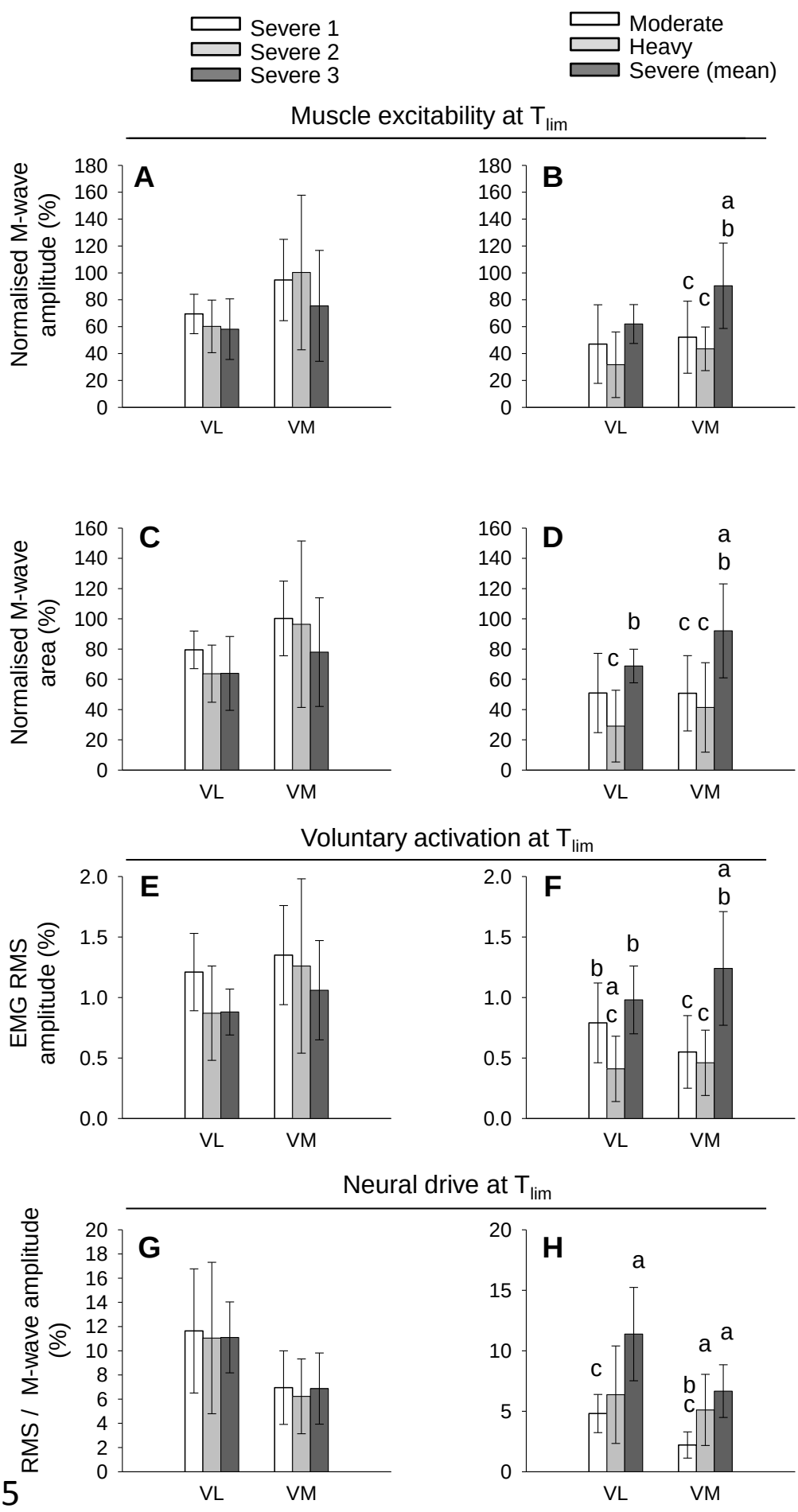
Severe 1
Severe 2
Severe 3
Moderate
Heavy
Severe (mean)
Muscle excitability at T_{lim}
Normalised M-wave amplitude (%)
A
B
Normalised M-wave area (%)
C
D
Voluntary activation at T_{lim}
EMG RMS amplitude (%)
E
F
Neural drive at T_{lim}
RMS / M-wave amplitude (%)
G
H
VL
VM

Figure 5

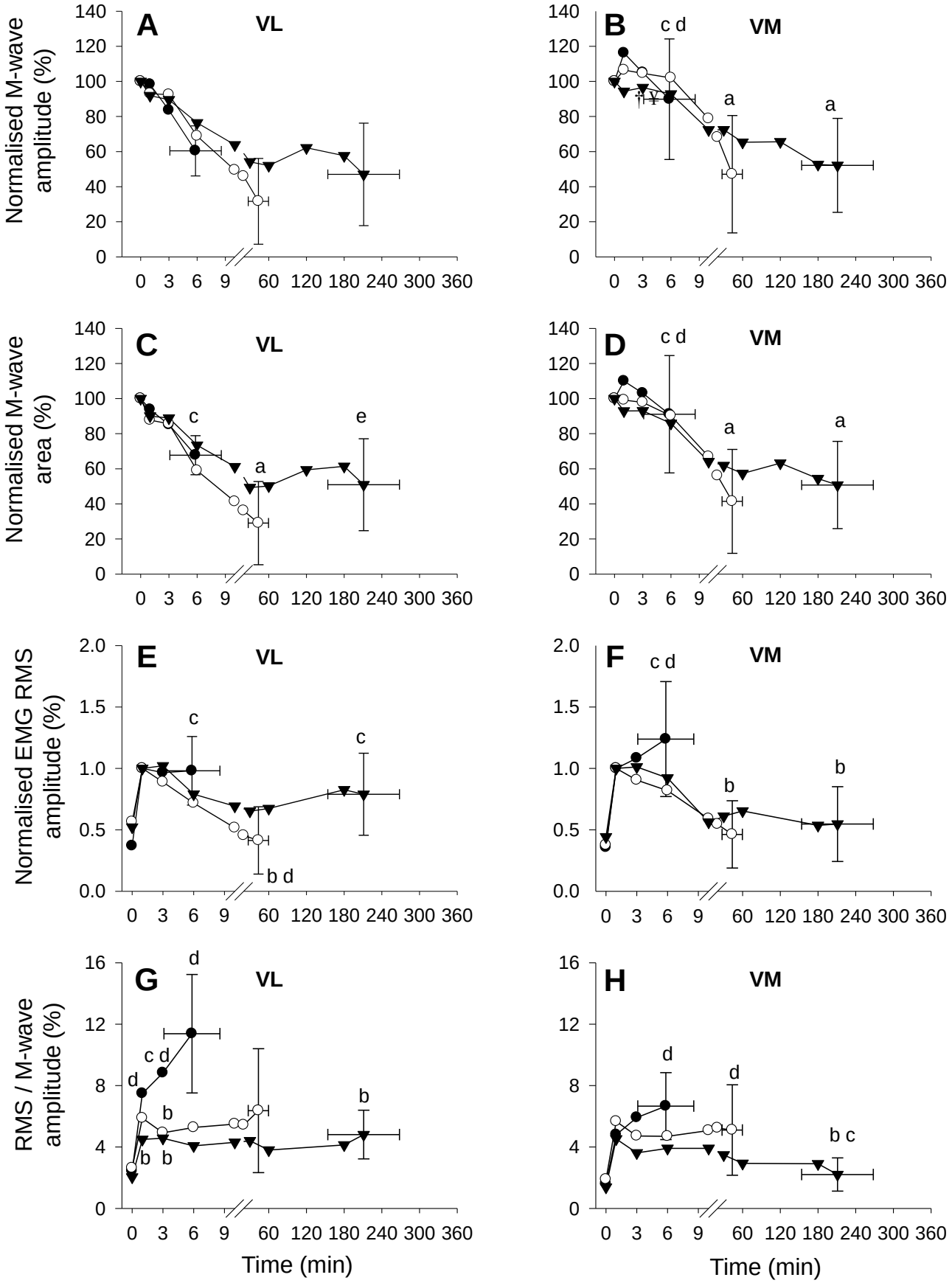
A
VL
B
VM
C
VL
D
VM
E
VL
F
VM
G
VL
H
VM
Normalised M-wave amplitude (%)
Normalised M-wave area (%)
Normalised EMG RMS amplitude (%)
RMS / M-wave amplitude (%)
Time (min)
Time (min)
0 3 6 9 60 120 180 240 300 360

Figure 6